Thin Solid Films xxx (2016) xxx–xxx

Contents lists available at ScienceDirect

Thin Solid Films

journal homepage: www.elsevier.com/locate/tsf

Effect of Sn/Zn/Cu precursor stack thickness on two-step processed kesterite solar cells

Samaneh Ranjbar [a,d,e,*], Guy Brammertz [b,c], Bart Vermang [d,e], Afshin Hadipour [d], M. Sylvester [b,d,e], Aniket Mule [d,e,f], Marc Meuris [b,c], A.F. da Cunha [a], Jef Poortmans [c,d,e]

[a] I3N - Departamento de Física, Universidade de Aveiro, Campus Universitário de Santiago, 3810-193 Aveiro, Portugal
[b] imec division IMOMEC - partner in Solliance, Wetenschapspark 1, 3590 Diepenbeek, Belgium
[c] Institute for Material Research (IMO), Hasselt University, Wetenschapspark 1, 3590 Diepenbeek, Belgium
[d] imec-partner in Solliance, Kapeldreef 75, 3001 Leuven, Belgium
[e] Department of Electrical Engineering (ESAT), KU Leuven, Kasteelpark Arenberg 10, 3001 Heverlee, Belgium
[f] Department of Mechanical and Process Engineering (D-MAVT), ETH Zurich, LEEK, Leonhardstrasse 21, 8092 Zurich, Switzerland

ARTICLE INFO

Article history:
Received 9 May 2016
Received in revised form 19 September 2016
Accepted 20 September 2016
Available online xxxx

Keywords:
Kesterite
Solar cells
Copper zinc tin selenide
Tin/Zinc/Copper precursor
Precursor thickness
Absorber layer
Thickness

ABSTRACT

We have fabricated $Cu_2ZnSnSe_4$ (CZTSe) solar cells with different absorber layer thickness. Absorber layers with different thicknesses were fabricated by changing the thickness of e-beam evaporated Sn/Zn/Cu precursor stacks and then selenization in a rapid thermal processing system. Scanning electron microscopy revealed that by increasing the thickness the morphology of CZTSe films improves substantially and energy dispersive spectrometry measurements showed that the Cu to Sn ratio increased with increasing the film thickness, despite a similar Cu to Sn ratio in the starting layers. A longer minority carrier lifetime and higher open circuit voltage were achieved for solar cells with thicker absorber layers. A maximum conversion efficiency of 7.8% (without anti reflection coating) was achieved for a solar cell with 1.7 μm thickness in which a low doping density of the order of 10^{15} cm^{-3} was measured, leading to a wide space charge region of about 300 nm.

1. Introduction

Kesterite compound $Cu_2ZnSn(S,Se)_4$, CZTSSe is being investigated as a promising candidate for cost effective thin film solar cells. In addition of desirable photovoltaic properties such as high absorption coefficient ($>10^4$ cm^{-1}) and optimal band gap (1–1.5 eV depending on the S/Se composition ratio), CZTSSe consists of inexpensive and abundant elements [1]. So far 12.6% conversion efficiency has been achieved for a CZTSSe solar cell synthesized by a hydrazine solution based process [2]. The effect of variation of thickness of absorber layer has been studied for pure sulfide Cu_2ZnSnS_4 [3]. In this study, we fabricated pure selenide $Cu_2ZnSnSe_4$ (CZTSe) solar cells by selenization of e-beam evaporated Sn, Zn and Cu layers. CZTSe absorber layers with different thicknesses were fabricated by changing the thickness of Sn/Zn/Cu precursor stacks and physical, optical and electrical properties of the solar cells were investigated.

2. Experimental details

Pure $Cu_2ZnSnSe_4$ (CZTSSe) absorber layers were synthesized in a two-step process. First, Sn, Zn and Cu were subsequently deposited on Mo-coated Soda Lime Glass (SLG) by e-beam evaporation. Metallic layers with different thickness (see Table 1) were deposited while the metallic ratios were kept constant in order to control the composition. In the second step, the Sn/Zn/Cu stacks were selenized by 10% H_2Se gas diluted in N_2 for 15 min at 460 °C in a rapid thermal processing system with 1 °C/s heating rate. This selenization process has been already optimized and applied for sputtered $Cu_{10}Sn_{90}$/Zn/Cu stack layers [4]. Absorber layers with thicknesses of ~300, 700, 1000, 1200 and 1700 nm were fabricated. These absorber layers were etched in 5% KCN solution for 2 min. KCN etching is beneficial for improving the performance of the CZTSe solar cells because it removes secondary phases such as Cu_xSe, SnSe, Se and oxides such as SnO as demonstrated in [5]. Solar cells were then completed by successive chemical bath deposition of CdS (~50 nm), sputtering of intrinsic ZnO (~50 nm) and Al-doped ZnO (~300–400 nm) and finally evaporation of Ni/Al grids. Solar cells with 0.5 cm^2 area were isolated by needle scribing of the devices. Top view scanning electron microscopy (SEM) and energy dispersive spectrometry (EDS) of the absorbers were acquired using a TESCAN Vega 3

* Corresponding author at: Department of Electrical Engineering (ESAT), KU Leuven, Kasteelpark Arenberg 10, 3001 Heverlee, Belgium.
E-mail address: samanehranjbarr@gmail.com (S. Ranjbar).

http://dx.doi.org/10.1016/j.tsf.2016.09.040
0040-6090/

Table 1
Metal composition of CZTSe absorbers with different thickness.

Thickness (nm) Sn/Zn/Cu	Thickness (nm) after selenization	Cu/Zn	Cu/Sn	Zn/Sn	Cu/(Sn + Zn)
54/26/30	300	1.97	1.24	0.63	0.76
107/53/60	730	1.34	1.38	1.03	0.68
215/105/120	1000	1.51	1.59	1.06	0.77
260/126/145	1200	1.49	1.59	1.07	0.77
310/150/160	1700	1.71	1.74	1.04	0.86

SBH equipped with a Bruker EDS system. The thickness of the samples was measured by cross sectional SEM images using a Nova 200 FEI tool. The electrical characterization of the solar cells were studied by light and dark current–voltage (I—V) using an Oriel solar simulator system with an AM1.5 G spectrum and 1 sun illumination. Capacitance-Voltage (C-V) were measured with an Agilent 4980A LCR-meter as a function of frequency varying from 10 kHz to 100 kHz and bias voltage from −2 V to 0.5 V, while AC voltage was 30 mV. Low injection time resolved photoluminescence (TR-PL) measurements were acquired at room temperature using a Hamamatsu C12132. A 532 nm pulsed laser with repetition rate of 15 kHz and average power density of 14 mW/cm^2 was used in this study.

3. Results and discussion

3.1. Morphological analysis

Top-view SEM images of CZTSe absorber layers with different thickness are shown in Fig. 1a–d and cross-sectional SEM images of devices with 700 nm and 1700 nm thickness are shown in Fig. 1e and Fig. 1f, re-

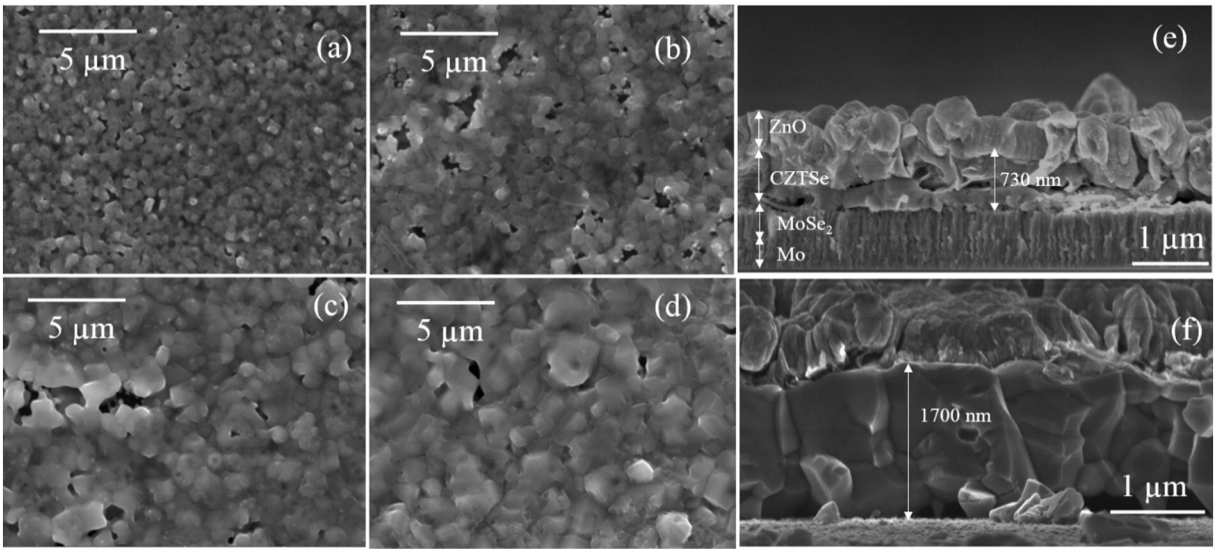

Fig. 1. Top view SEM images of absorber layers: (a) to (d) absorbers with 300, 700, 1200, and 1700 nm thickness, respectively. (e) and (f) cross section SEM images of solar cells with absorber layer thickness of 700 nm and 1700 nm.

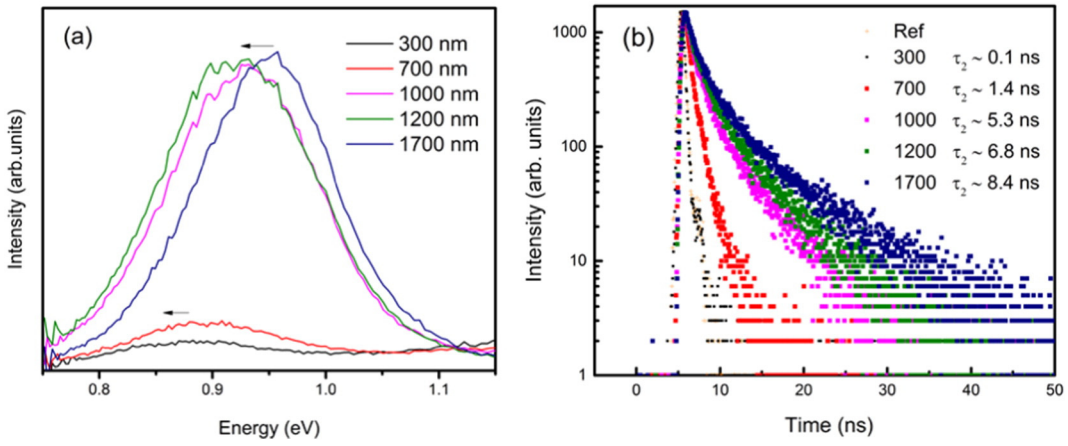

Fig. 2. (a) Photoluminescence spectra and (b) time resolved Photoluminescence spectra of solar cells with different absorber thickness. Minority carrier lifetime (τ) is derived from a two exponential fit.

Please cite this article as: S. Ranjbar, et al., Effect of Sn/Zn/Cu precursor stack thickness on two-step processed kesterite solar cells, Thin Solid Films (2016), http://dx.doi.org/10.1016/j.tsf.2016.09.040

Table 2
Electrical and optical parameters of solar cells with different absorber thickness: short circuit current (J_{sc}), open circuit voltage (V_{oc}), fill factor (FF), efficiency (η), shunt resistance (R_{sh}) and series resistance (R_s) are derived from illuminated current-voltage (J-V) measurement, J_{sc} (EQE) are derived from external quantum efficiency (EQE). PL peak position (PL) is derived from photoluminescence measurement.

Thickness (nm)	J_{sc} (mA/cm^2)	J_{sc} (EQE) (mA/cm^2)	V_{oc} (mV)	FF (%)	η (%)	R_{sh} ($\Omega\cdot$cm^2)	R_s ($\Omega\cdot$cm^2)	PL (eV)
300	2.3	_	175.0	25	0.1	68	2.07	0.89
730	15.2	_	262.0	34	1.4	31	1.16	0.89
1000	26.9	26.60	363.0	47	4.6	98	1	0.93
1200	30	34.92	385.0	54	6.2	277	1.26	0.91
1700	36.4	39.50	406.0	53	7.8	512	1.35	0.95

spectively. SEM images reveal that by increasing the thickness the morphology of the absorbers improves, the grain size increases and less voids and pinholes can be observed in the films.

The composition of the samples was measured by EDS and the results are given in Table 1. Although the metallic ratios were kept constant in order to control the composition and X-ray fluorescence measurement of initial precursors confirmed the expected thicknesses for all samples, the Cu/Sn decreases constantly by decreasing the thickness. The reason of Sn excess composition of the thinner samples is not quite clear, however, the faster interdiffusion of the three metal layers and consequently reduced formation of volatile $SnSe_2$ might be the reason for larger amount of Sn in the thinner samples as compared to the thicker samples.

3.2. Optical and electrical characterization

Fig. 2a shows the room temperature photoluminescence (PL) of the solar cells. The position of the PL peak of the solar cells with different thickness is summarized in Table 2. By decreasing the thickness, the PL spectra become broader and the PL peak position shifts towards lower energies. This red shift is more significant for ultra-thin samples (≤700 nm) and can be attributed to the composition variation. The PL peak of CZTSe is generally attributed to a donor to acceptor recombination in the presence of a large amount of band tail states and potential fluctuations [6]. The larger number of tail states in thinner samples may be due to several reasons such as the Sn rich composition which can lead to formation of Sn_{Cu} and Sn_{Zn} deep donors, or the formation of secondary phases with different band gaps that produce band tails.

Fig. 2b shows the minority carrier lifetime (τ_2) of solar cells with different thickness. The minority carrier lifetime is derived using a two exponential fit to the photoluminescence decay curve. The slower decay time usually is considered as the minority carrier lifetime [7]. The minority carrier lifetime of the samples increases by increasing the thickness and it reaches 8.4 ns when thickness of absorber layer is 1700 nm. The minority carrier lifetime variation can be correlated to the variation of the carrier concentration or composition mainly in ultra-thin samples in which Sn-rich composition could lead to formation of electron trapping defects such as Sn_{Cu}. Another possibility could be the existence of voids and secondary phases at the Mo rear interface. These imperfections are very likely at the rear interface due to the decomposition reaction during the annealing step [8,9]. By increasing the thickness of the absorber layer the distance between the p-n junction and the rear surface increases and the detrimental effects of the imperfections will be suppressed to some extent.

Fig. 3 shows the carrier concentration profile of the absorbers with different thicknesses obtained by Mott-Schottky plot from the C—V measurement at frequency of 40 kHz. By increasing the thickness, the doping density (N_a) at the edge of space-charge region (SCR), decreases substantially, thus the SCR becomes wider. The reason for this large variation in doping density is not quite clear but might be related to the variation of the composition. As Fig. 6a shows by increasing the thickness the Cu to Sn ratio increases while the doping density decreases significantly. In addition by increasing the thickness the p-n junction will

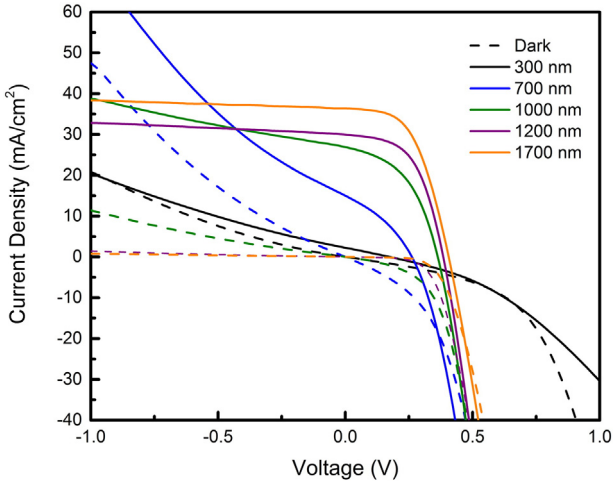

Fig. 4. Current-voltage measurement of solar cells with different absorber thickness under dark (dashed line) and 1 sun illumination (solid line).

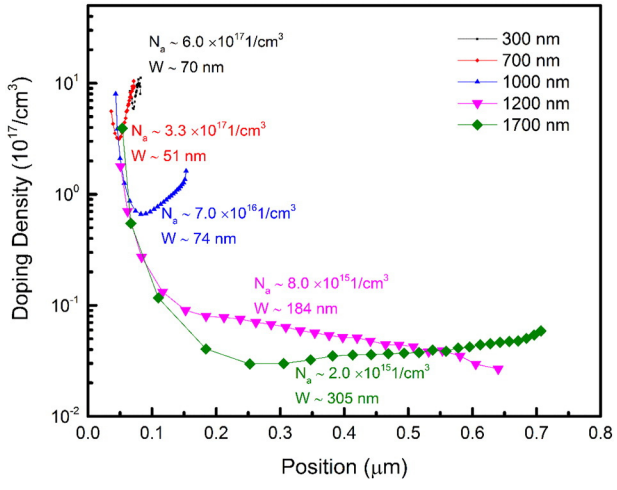

Fig. 3. Doping density profile of solar cells with different absorber thickness. The hole concentaration (N_a) and space charge region width (W) are derived from Mott–Schottky plot.

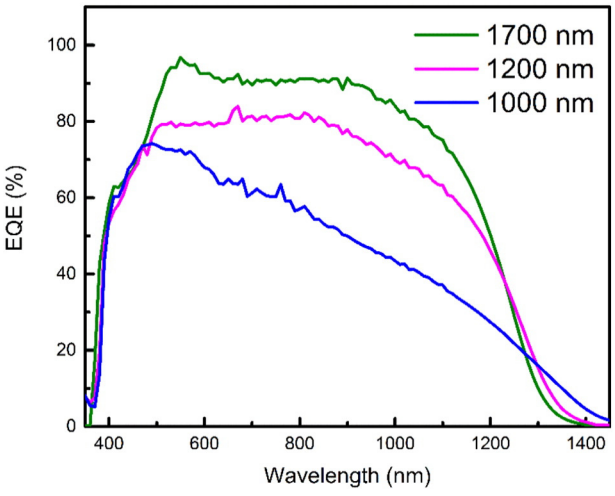

Fig. 5. External quantum efficiency (EQE) of solar cells with different absorber layer thickness.

Please cite this article as: S. Ranjbar, et al., Effect of Sn/Zn/Cu precursor stack thickness on two-step processed kesterite solar cells, Thin Solid Films (2016), http://dx.doi.org/10.1016/j.tsf.2016.09.040

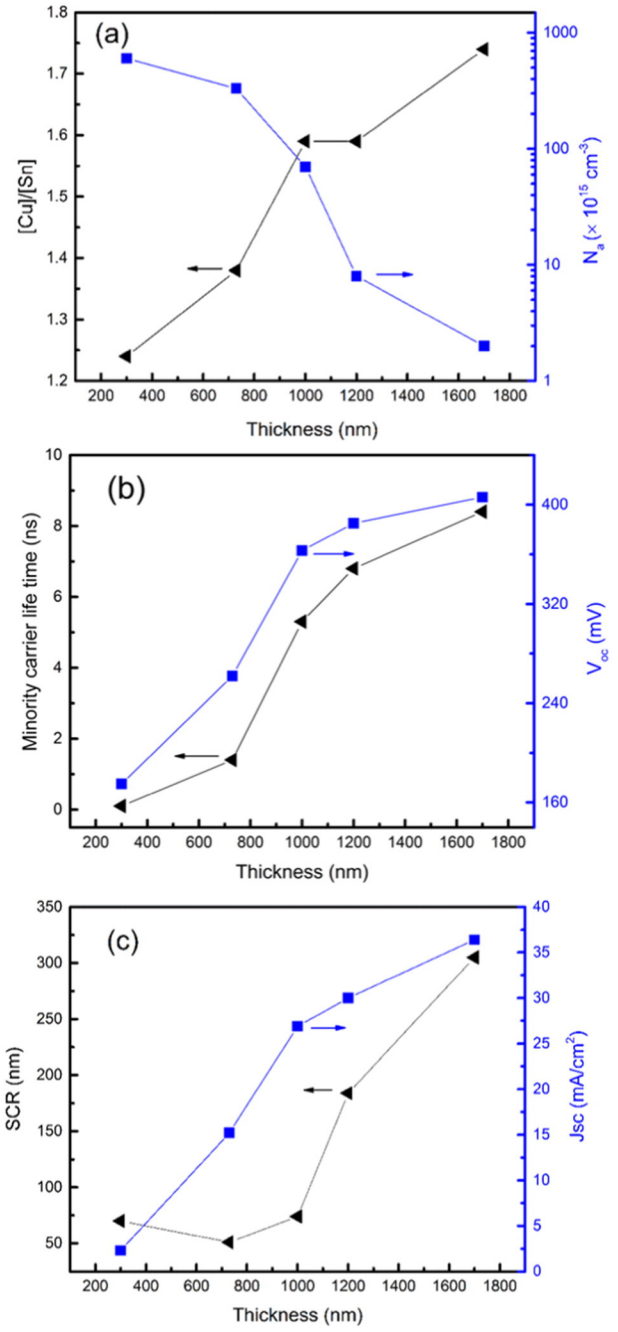

Fig. 6. (a) Cu to Sn ratio and hole concentration (N_a), (b) Minority carrier lifetime and V_{oc}, (c) Depletion width (SCR) and J_{sc} at various thickness.

be less affected by the imperfections at the rear contact and less defects can diffuse to this region where we measure the carrier concentration. Another possibility could be the contribution of elements that diffuse in from the SLG for example alkali elements. By increasing the thickness the diffusion of these elements to the p-n junction will be reduced.

Fig. 4 shows the illuminated/dark I-V curve (solid/dashed lines) of the champion solar cells of each thickness. The corresponding cell parameters are derived from the procedure explained by Hegedus and Shafarman [8] and are summarized in Table 2. Shunt resistance (R_{sh}) is very low when the absorber thickness is ≤1000 nm and it improves significantly to 512 Ω·cm^2 for the thickest sample since the film becomes more compact. Short circuit current (J_{sc}) is very low when the thickness of the device is ≤1000 nm because of the incomplete collection of solar spectrum. Further improvement of J_{sc} of samples thicker than 1000 nm can be attributed to a wider SCR that facilitate the collection of carriers. Fig. 6c shows that by increasing the thickness from 1000 nm to 1700 nm the SCR increases from 70 nm to 300 nm and J_{sc} improves up to 36.4 mA/cm^2. The significant improvement of open circuit voltage (V_{oc}) by increasing the thickness indicates the reduction of recombination currents and it is consistent with the enhancement of minority carrier lifetime (see Fig. 6b).

Finally, external quantum efficiency (EQE) measurements shown in Fig. 5 indicate that by increasing the thickness photocurrent collection improves mainly due to the wider SCR and the longer minority carrier lifetime.

4. Conclusions

In conclusion, increasing the thickness of Sn/Zn/Cu precursor stacks improved the quality and morphology of CZTSe absorber layers prepared by selenization of e-beam evaporated precursors. Despite a similar composition in the starting layers, selenization of the thicker metal starting layers led to a larger Cu to Sn ratio in the final absorber, possibly because the thinner starting layers show faster interdiffusion of the metals and suppressed $SnSe_2$ evaporation. The enhanced physical quality of the absorber layers leads to higher performance of solar cells, especially due to a, longer minority carrier lifetime and accordingly higher V_{oc}. In addition, it was found that the doping of the absorber layer decreased with increasing the thickness and the wider space charge region of the thicker devices leads to better collection of photogenerated carriers and higher J_{sc}.

Acknowledgements

This project has received funding from the European Union's Horizon 2020 research and innovation programme under grant agreement No 640868. This research is partially funded by the Flemish government, Department Economy, Science and innovation. This work is also funded by FEDER funds through the COMPETE 2020 Programme and National Funds through FCT - Portuguese Foundation for Science and Technology under the project UID/CTM/50025/2013. Samaneh Ranjbar acknowledges the financial support of the Portuguese Science and Technology Foundation (FCT) through PhD grant SFRH/BD/78409/2011.

References

[1] S. Delbos, K¨esterite thin films for photovoltaics: a review, EPJ Photovolt. 3 (2012) 35004–35016.
[2] W. Wang, M.T. Winkler, O. Gunawan, T. Gokmen, T.K. Todorov, Y. Zhu, D.B. Mitzi, Device characteristics of CZTSSe thin-film solar cells with 12.6% efficiency, Adv. Energy Mater. 4 (2014) 1301465–1301469.
[3] Y. Ren, J.J. Scragg, C. Frisk, J.K. Larsen, S.Y. Li, C. Platzer-Björkman, Influence of the Cu_2ZnSnS_4 absorber thickness on thin film solar cells, Phys. Status Solidi A 212 (2015) 2889–2896.
[4] G. Brammertz, M. Buffière, S. Oueslati, H. ElAnzeery, K. Ben Messaoud, S. Sahayaraj, C. Köble, M. Meuris, J. Poortmans, Characterization of defects in 9.7% efficient $Cu_2ZnSnSe_4$–CdS–ZnO solar cells, Appl. Phys. Lett. 103 (2013) 163904–163907.
[5] M. Buffière, G. Brammertz, S. Sahayaraj, M. Batuk, S. Khelifi, D. Mangin, A.-A. El Mel, L. Arzel, J. Hadermann, M. Meuris, J. Poortmans, KCN chemical etch for Interface engineering in $Cu_2ZnSnSe_4$ solar cells, ACS Appl. Mater. Interfaces 7 (2015) 14690–14698.
[6] S. Oueslati, S. Oueslati, G. Brammertz, M. Buffière, C. Köble, T. Oualid, M. Meuris, J. Poortmans, Photoluminescence study and observation of unusual optical transitions in $Cu_2ZnSnSe_4$/CdS/ZnO solar cells, Sol. Energy Mater. Sol. Cells 134 (2015) 340–345.
[7] D.H.L. Kanevce, D. Kuciauskas, The role of drift, diffusion, and recombination in time resolved photoluminescence of CdTe solar cells determined through numerical simulation, Prog. Photovolt. Res. Appl. 22 (2014) 1138–1146.
[8] J.J. Scragg, J.T. Wätjen, M. Edoff, T. Ericson, T. Kubart, C. Platzer-Björkman, A detrimental reaction at the molybdenum back contact in $Cu_2ZnSn(S,Se)_4$ thin-film solar cells, J. Am. Chem. Soc. 134 (2012) 19330–19333.
[9] J.J. Scragg, T. Kubart, J.T. Watjen, T. Ericson, M.K. Linnarsson, C. Platzer-Björkman, Effects of back contact instability on Cu_2ZnSnS_4 devices and processes, Chem. Mater. 25 (2013) 3162–3171.

Please cite this article as: S. Ranjbar, et al., Effect of Sn/Zn/Cu precursor stack thickness on two-step processed kesterite solar cells, Thin Solid Films (2016), http://dx.doi.org/10.1016/j.tsf.2016.09.040